Relationship between Wind and Precipitation Observed with a UHF Radar, GPS Rawinsondes and Surface Meteorological Instruments at Kototabang, West Sumatera during September–October 1998

Fumie MURATA, Manabu D. YAMANAKA[1]

Graduate School of Science and Technology, Kobe University, Kobe, Japan

Masatomo FUJIWARA[2]

Graduate School of Environmental Earth Science, Hokkaido University, Sapporo, Japan

Shin-Ya OGINO[3]**, Hiroyuki HASHIGUCHI, Shoichiro FUKAO**

Radio Science Center for Space and Atmosphere, Kyoto University, Uji, Japan

Mahally KUDSY, Tien SRIBIMAWATI, Sri Woro B. HARIJONO

Agency for the Assessment and Application of Technology (BPPT), Jakarta Pusat, Indonesia

and

Eddy KELANA

Indonesian Meteorological and Geophysical Agency (BMG), Jakarta Pusat, Indonesia

(Manuscript received 25 May 2000, in revised form December 2001)

Abstract

Simultaneous observations with a UHF-band boundary layer radar (hereafter referred as BLR), GPS rawinsondes and a tipping-bucket-type rain gauge were conducted at Kototabang (0.20°S, 100.32°E, 865 m MSL), which is located on the mountainous region near Bukittinggi, West Sumatera Province, during 27 September–7 October 1998 (rainy season). Low-level (1–3 km) westerly wind stronger than 10 m/s was observed, and precipitation tended to occur when the low-level westerly wind became weak (2–5 October). Similar relationship was observed for two months (1 September–31 October 1998) during which only BLR and surface meteorological instruments were operated at Kototabang. NCEP/NCAR

Corresponding author: Fumie Murata, Graduate School of Science and Technology, Kobe University, 1-1 Rokkoudaimachi, Nada-ku, Kobe 657-8501, Japan.
E-mail: murata@ahs.scitec.kobe-u.ac.jp

1 Second affiliation: Frontier Observation Research System for Global Change, Hamamatsucho, Tokyo 105-0013, Japan

2 Present affiliation: Radio Science Center for Space and Atmosphere, Kyoto University, Uji, Kyoto 611-0011, Japan

3 Present affiliation: Graduate School of Science and Technology, Kobe University, Kobe, Hyogo 657-8501, Japan

objective analysis, and GMS T_{BB} data showed that the low-level (850 hPa) wind field, and cloud distribution, were both completely different between the Indonesian Archipelago (east of Kototabang) and the eastern Indian Ocean—including the Bay of Bengal (west of Kototabang)—during the analysis period. Two large-scale cloud disturbances existed along the equator in the western side (80°–100°E), but precipitation at Kototabang did not correspond to these cloud disturbances. The implication is that effects of the mountain range of Sumatera blocked the large-scale cloud disturbances over the Indian Ocean. The precipitation by local-scale cloud systems prevailed at Kototabang. The convergences of local circulations, which are generally dominant under weak background winds, are considered as the major cause of local-scale cloud systems.

1. Introduction

Convection plays the most important role in the tropical atmospheric dynamics. Abundant heat and moisture provided from the ocean cause active convections. The temporal scale of the tropical convective cloud systems ranges from 1–2 days (corresponding to cloud clusters), to 30–60 days (often called the intraseasonal oscillations (ISO), which was first suggested by Madden and Julian (1971)). These disturbances often have the structures of theoretical equatorial waves (e.g., Takayabu 1994). Nakazawa (1988) showed that these disturbances (with different scales) interact with each other, and are organized to be a hierarchical structure. Displacements and activities of these multi-scale convective systems trigger the onset and break up of El Niño events (e.g., Lau et al. 1989). Furthermore it is suggested that the smaller-scale disturbances which develop under local weather and/or geographical conditions (e.g., Nitta and Sekine 1994) may influence the global-scale phenomena, such as El Niño events through the hierarchical structure.

The Indonesian maritime continent is located in the 'warm pool' region where the sea surface temperature is the highest all over the world. As the land-sea distribution is complicated over the Indonesian maritime continent, cloud systems may be controlled by different factors in different regions within the continent. Nitta et al. (1992) analyzed the geostationary meteorological satellite (GMS) observation data, and pointed out that cloud disturbances moving eastward from the Indian ocean are strongly modified, or re-organized, near Sumatera Island—which is located at the western end of the archipelago. However, no detailed observations have been carried out in Sumatera Island. Although Hamada et al. (2002) have collected and analyzed daily rainfall amount data over Indonesia including Sumatera Island, they did not show the mechanism to develop or modify the cloud systems, mainly because information on the distributions of wind, temperature, humidity and their time evolutions associated with the cloud systems was quite insufficient.

In August 1998 a boundary layer radar (hereafter referred as 'BLR') was installed at Kototabang near Bukittinggi, West Sumatera Province (0.20°S, 100.32°E, 865 m MSL) (Fig. 1). BLR is a 1.3 GHz wind profiler, with which we can observe horizontal wind velocity until about 6.5 km above the ground. It detects the precipitation particle motion on rainy conditions, and the atmospheric motion on clear conditions. A similar type of BLR has been operated at Serpong near Jakarta, West Java of Indonesia (6.4°S, 106.7°E) (Fig. 1) since November 1992, and several studies related to cloud convection systems have been carried out (Hashiguchi et al. 1995, 1996; Widiyatmi et al. 1999). At Kototabang, the first intensive observation had been conducted with BLR, GPS rawinsondes, ozonesondes and a tipping-bucket-type rain gauge during 27 September–7 October 1998 in collaboration with Kobe University, Kyoto University and the University of Tokyo, Japan and BPPT (Agency for Assessment and Application of Technology) and BMG (Indonesian Meteorological and Geophysical Agency), Indonesia.

The main aims of this paper are to describe the observational results at Kototabang, and discuss the development, and/or modification mechanisms, of cloud systems in Sumatera Island. In Section 2 the observation instrumentation and the other data used in this study are described. In Section 3 the determination of precipitation based on the BLR observations is discussed. In Sections 4 and 5 results of the ob-

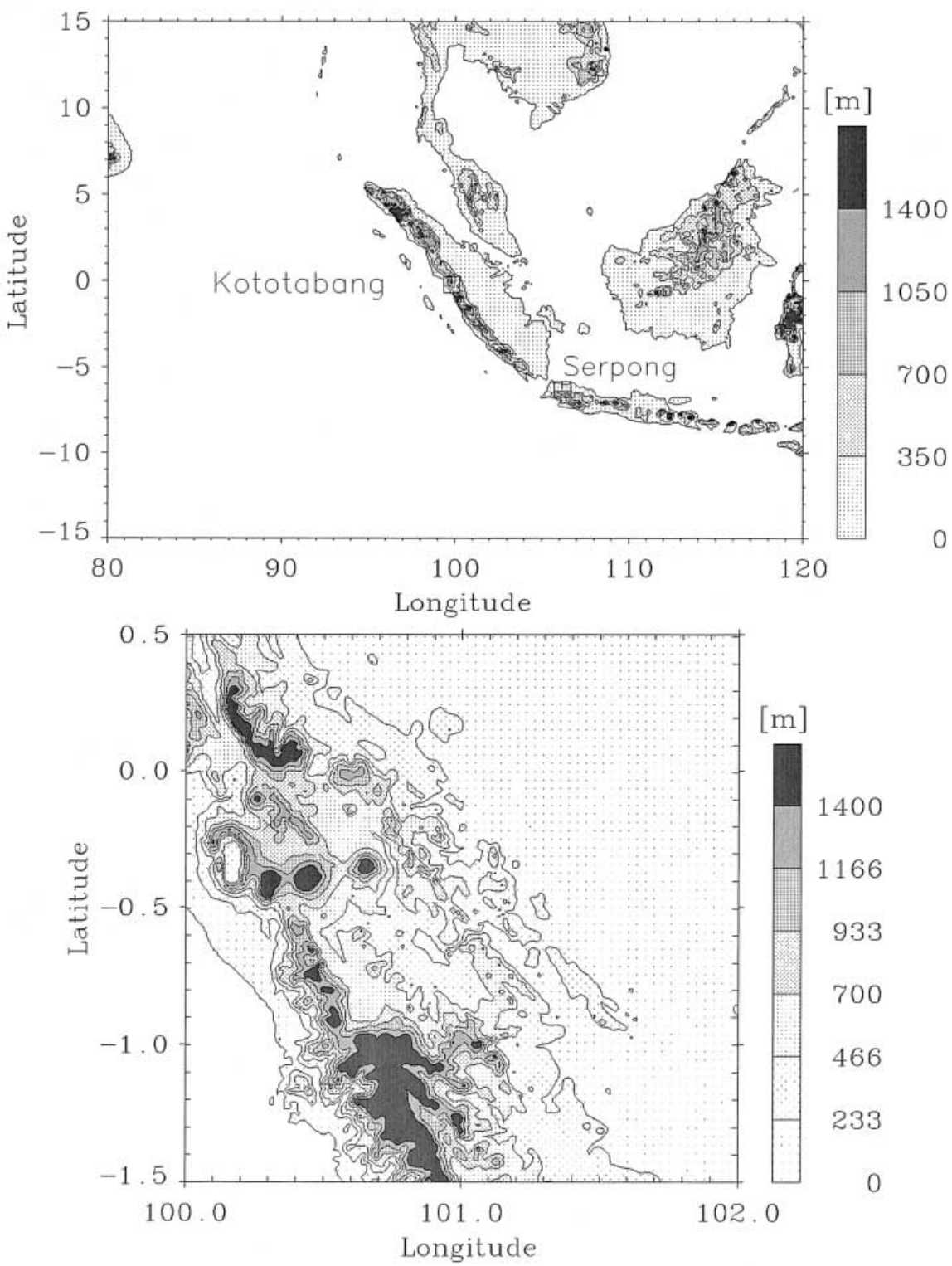

Fig. 1. Upper panel is a geographical map of BLR sites. Lower panel is a geographical map of around Kototabang (100.3°E, 0.2°S). The data were downloaded from the internet site of the U.S. Geological Survey (http://www.edcdaac.usgs.gov/gtopo30/gtopo30.html).

servations and data analyses are described. In Section 6 some plausible mechanisms to explain the observational features are discussed. Section 7 is the conclusion of this paper.

2. Observation and data description

The intensive observation was carried out during 27 September–7 October 1998 at Kototabang. This period corresponds to one of two rainy seasons during September–November, and March–May in the central part of Sumatera (Hamada et al. 2002), which appear due to the annual variation (north–south movement around the equator) of the inter–tropical convergence zone (ITCZ) (Murakami and Matsumoto 1994). It was the first observation campaign of BLR (see Subsection 2.1) since its installation in August 1998, GPS rawinsondes (Subsection 2.2), ozonesondes (which were not utilized in this paper), and a rain gauge (Subsection 2.3) were operated during this campaign period.

At Kototabang a Global Atmosphere Watch (GAW) Station of World Meteorological Organization (WMO) was constructed in 1996. We utilized data of the surface meteorological instruments installed there (Subsection 2.4), as well as the BLR data, during September–October 1998. We also used some database (Subsection 2.5) in order to obtain larger-scale information.

2.1 Boundary layer radar (BLR)

BLR transmits radio waves with frequency of 1357.5 MHz (UHF or *L*-band), of which clear-air echoes are induced by the refractive index fluctuations due to atmospheric turbulence, and spatial differences of temperature and humidity (see e.g., Gage et al. 1990), and they provide information on atmospheric motions in clear air by the Doppler principle. The radio waves with this frequency band are reflected with much greater echo intensity for precipitation particles than for the atmosphere during rainfall. Because the vertical Doppler velocity due to falling precipitation particles is as large as several m/s, it can be distinguished from the atmospheric vertical motion (normally less than 1 m/s). For these reasons, the rainfall duration has been determined by the data of BLR vertical Doppler velocity and BLR echo power, as will be described in Section 3.

BLR has been operated continuously since its installation, except for short periods of the electric power shortage. The time resolution is about 1 minute, the vertical resolution is about 100 m, and the sampling height range is up to 6.5 km height. Further details on BLR have been described in Hashiguchi et al. (1995, 1996) and Renggono et al. (2001).

2.2 GPS rawinsonde measurement

GPS rawinsondes provide vertical profiles of pressure, temperature, humidity and horizontal wind. We employed an AIR GPSonde sounding system with meteorological balloons (TA-1000 type for daytime, and TX-1000 for nighttime) provided by TOTEX Co. Ltd.. They were launched four times a day at 0030, 0630, 1230 and 1830 LST (corresponding to observations for 1800, 0000, 0600 and 1200 GMT, respectively), except for 27 and 28 September on which the launch was done once per day (1630 and 1230 LST, respectively). In this paper, the vertical coordinate is unified to a height from the BLR station, which is 865 m MSL.

2.3 Rain gauge measurement

We used a standard tipping-bucket-type rain gauge (produced by Ogasawara Co. Ltd.). The minimum sensitivity for rainfall amount was 0.5 mm, and the temporal resolution of the recorded data was 1 min. The rain gauge was put on the roof of the GAW station building, which was just on the neighborhood of the BLR antenna.

2.4 Surface measurements

The data of surface temperature, pressure, and relative humidity used in this study were provided from standard operational observations (barograph and thermohygrograph) at the GAW station. Two-month data during 00 LST on 1 September–23 LST on 31 October 1998 were used. They were sampled every hour on the hour.

2.5 Other data

The following data were utilized to obtain the horizontal distributions of cloud and wind during September–October 1998.

a. Satellite cloud data

The data of black body temperature (T_{BB}) by GMS IR1 sensor were provided by JMA through the Disaster Prevention Research In-

stitute, Kyoto University. T_{BB} represents the cloud top temperature when an area with spatial resolutions of 0.2° in longitude and in latitude is covered by clouds, so that we can estimate the cloud top height. Lower T_{BB} values correspond to higher cloud tops. The temporal resolution is an hour.

b. Objective analysis data

Daily averaged 850 hPa wind data of NCEP/NCAR Reanalysis were downloaded from the following internet site:

http://wesley.wwb.noaa.gov/ncep_data/index_sgi62.html

courtesy of the US National Weather Service. The spatial resolution is 2.5° both in longitude and latitude.

3. Determination of rainfall durations

The precipitation echoes detected with BLR are much stronger than clear air echoes (Gage 1990; Hashiguchi et al. 1995; Renggono et al. 2001). The BLR Doppler velocity due to falling precipitation particles becomes as large as several m/s, which is much larger than that of usual atmospheric vertical motion. Consequently, rainfall can be detected by using both the echo power intensity, and the vertical Doppler velocity observed with BLR. Algorithms to distinguish precipitation echoes from atmospheric echoes by the magnitude of echo power intensity have been developed at Kyoto University.[1]

The time interval and height range used for the determination of rainfall durations were selected by the following reasons: Ice crystals may exist above the melting layer at around 4 km. The observed radar echo intensity below 2 km is underestimated due to saturation in the dynamic range of the radar receiver. We selected 2–3 km as the height range for rainfall determination. The rainfall intensity by a tipping-bucket-type rain gauge, which was utilized to compare with BLR echoes, is determined on the assumption that the rainfalls occur uniformly during the counts of tipping of the bucket. The time resolutions (1 min) of both BLR and the rain gauge are too short for normal rainfall to full the volume (0.5 mm) of the rain gauge bucket, and the lifetime of a convective cloud is sufficiently within 1 hour. Consequently, we took 10 min as the time interval for rainfall determination.

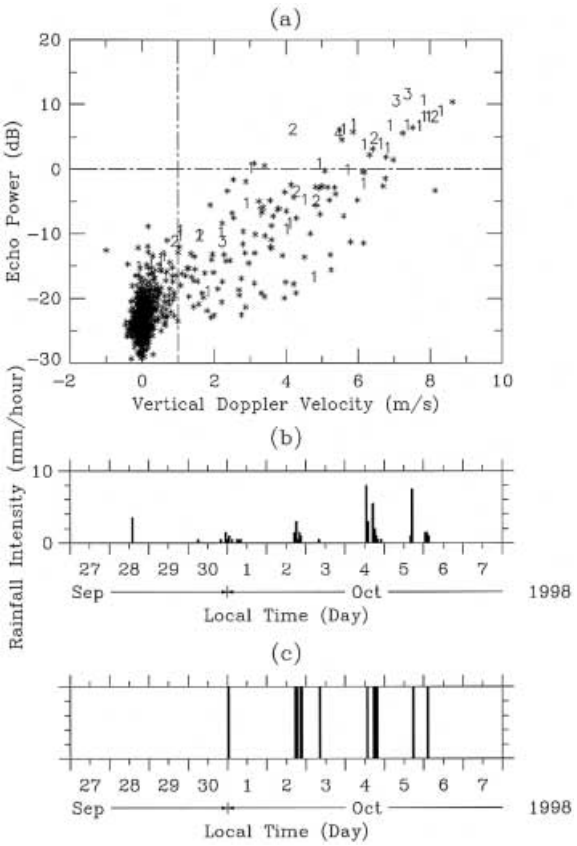

Fig. 2. (a) A distribution of BLR vertical Doppler velocity versus BLR echo power intensity during the intensive observation period. Positive and negative values of the vertical Doppler velocity are downward and upward, respectively. Each point was the data averaged for 2–3 km in height and for 10 min in time. '1', '2', '3' and '4' denote rainfall intensities (observed by a rain gauge simultaneously) of 0.5–1.0, 1.0–3.0, 3.0–6.0 and ≥6.0 mm/10 min. (b) Rainfall amount (per hour) by the rain gauge. (c) Rainfall durations decided by BLR. These are shown every hour, which contain more than one decided rainfall durations by every 10 min.

Figure 2a shows the distribution of vertical

1 Tan, T.K., 1995: A study on the algorithm for distinction of non-atmospheric echoes observed with an *L*-band clear-air doppler radar. Bachelor's thesis, Department of Electronic Engineering, Kyoto university, 38pp.

Doppler velocity versus echo power intensity during the intensive observation period. Positive and negative values of the vertical Doppler velocity are downward and upward, respectively. Each data sample was averaged for 2–3 km in height, and for 10 min in time. Remarkable rainfalls observed by the rain gauge simultaneously are also indicated. Weak echo power intensities concentrated near the zero Doppler velocity correspond to the clear air echoes. On the other hand, precipitation echoes have large Doppler velocities and show strong echo power intensities.

Based on this distribution, we determined threshold values to discriminate atmospheric and raindrop echoes as '0 dB' for the echo power, and '1 m/s' for the Doppler velocity. Figures 2b and 2c show a comparison between rainfall intensity observed by the rain gauge and the rainfall duration determined by the BLR echoes. Both the results are in good coincidence with each other. It should be mentioned that the BLR echo method is not always useful when the rainfall intensity is very weak, when the precipitating clouds have very low cloud-base (below 2 km), or when the precipitation occurs on a short time ($\ll$10 min).

Using the method mentioned above, the determination of precipitation durations is extended two months, September–October 1998 (see Fig. 4b of Section 4).

4. Correlation between precipitation and weak westerly wind

In this section results of data obtained at Kototabang are described. We mainly focus ourselves into a relationship between rainfall and wind variations, which is suggested first from results obtained during the two-week intensive observation period as will be described in Subsection 4.1. Next we extend the analysis period to the two months including the intensive observation period, and confirm the same relationship as will be described in Subsection 4.2.

4.1 Results for the intensive observation period

Figure 3 shows the results of the intensive observation with BLR, GPS rawinsondes and the rain gauge. Figures 3a and 3b are time-height cross sections of zonal wind observed by rawinsondes and by BLR, respectively. In this period westerly wind is dominant below 6 or 7 km, and is especially strong below 3 km. From 29 September to the daytime of 2 October, and after the daytime of 5 October, westerly wind stronger than 10 m/s appears below 3 km. Figures 3c and d are variations of BLR echo power and rain intensity by the rain gauge. Strong BLR echoes shown in the former correspond to heavy rain, as mentioned in Section 3. Precipitations do not occur every day, and that stronger than 2 mm/hour are concentrated during the afternoon of 2–5 October, which is the weak westerly period suggested in Figs. 3a and b. Therefore, the westerly wind variation is anti-correlated to precipitation. This is one of the most important results in this study, and will be examined again in the two-month data in Subsection 4.2.

Figure 3e shows time-height variation of equivalent potential temperature by rawinsondes. The equivalent potential temperature below 3 km generally shows convective instability during the intensive observation period. This is the typical stratification in the tropical region (see e.g., Fig. 11.1 of Holton 1992). During the weak westerly period the equivalent potential temperature is decreased uniformly in vertical, it implies that the atmosphere has been mixed by convection. When the westerly wind is strong, the equivalent potential temperature is minimum at 1–2 km.

4.2 Results for September–October 1998

Figure 4 shows the zonal wind variation (averaged over 1–2 km height range), and the rainfall durations observed by BLR during September–October 1998. The rainfall durations during the two months are also correlated to the weak westerly periods, as suggested in the two-week intensive observation period mentioned in Subsection 4.1. In particular, during 15 September–15 October, the zonal wind varies with a periodicity of about 10 days. The rainfall also has a similar periodicity.

Spectral analysis has been made to confirm the quasi-10-day periodicity. Figure 5 shows the energy-content form of power spectral densities calculated for zonal, and meridional, wind components averaged for 1–2 km height range during September–October 1998. A peak of 8–10 days is obvious for the zonal wind. The meridional wind also has a clear peak around

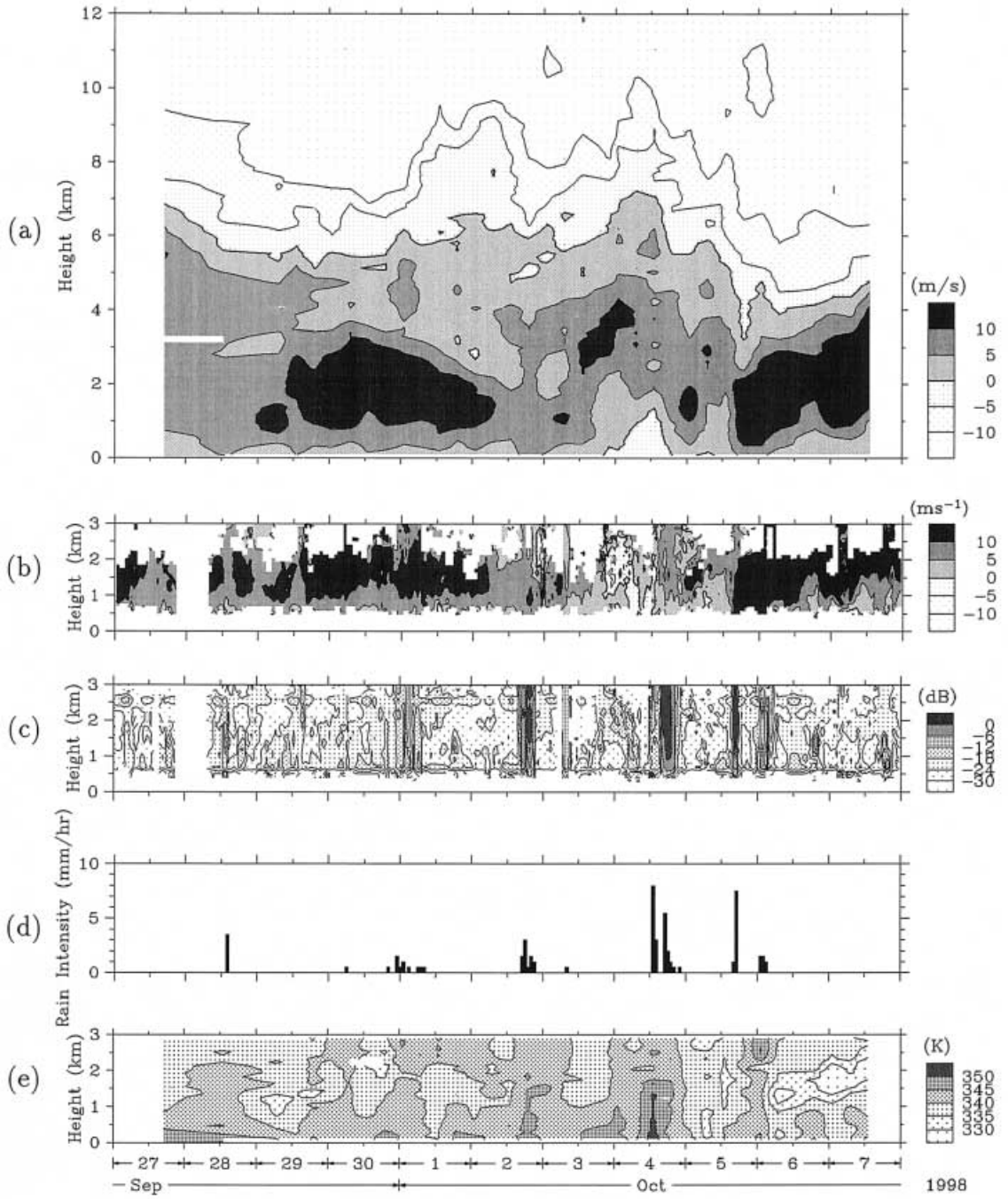

Fig. 3. Results of the intensive observation period during 27 September–7 October 1998. Time-height cross-sections of zonal wind observed (a) by rawinsondes launched 4 times per day, and (b) by BLR (60-min averaged). (c) 60-min averaged BLR echo power intensity. (d) Surface rainfall intensity observed by a rain gauge. (e) Time-height cross-section of equivalent potential temperature observed by rawinsondes.

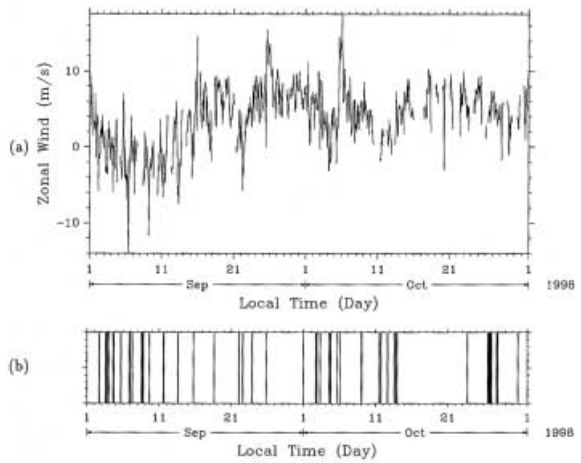

Fig. 4. Results of two months during September–October 1998. (a) Time series of 60-min averaged zonal wind (averaged over 1–2 km height range). (b) Rainfall durations decided by BLR.

10–20 days, but the spectral amplitude is much smaller than that of the zonal wind. The diurnal component of meridional wind variation has a similar amplitude to the quasi-10-day component, but that of zonal wind variation is weak. A 3–4 day component is also found for both the zonal and meridional winds.

Figure 6 shows frequency power spectral densities for surface pressure, temperature and specific humidity. For all the variables the diurnal component is dominant, and a periodicity of 2 days is found. Temperature and pressure have clear semi-diurnal periodicities, which may correspond to the atmospheric tide. A periodicity of 1.5 days appears in temperature and humidity, and a periodicity around 6 days is found for temperature. However, the 10-day component is generally very small in the surface meteorological quantities.

Therefore the spectral analyses for the lower-tropospheric wind, and the surface meteorological quantities, show existence of the diurnal component and the components with periods from a few days to about 20 days. After this we particularly notice the diurnal component, and the component of about 10 days, respectively.

On one hand, in order to examine the diurnal variation of rainfall, Fig. 7 shows a histogram of precipitation for each hour at Kototabang during September–October 1998. The precipitation periods were determined by BLR

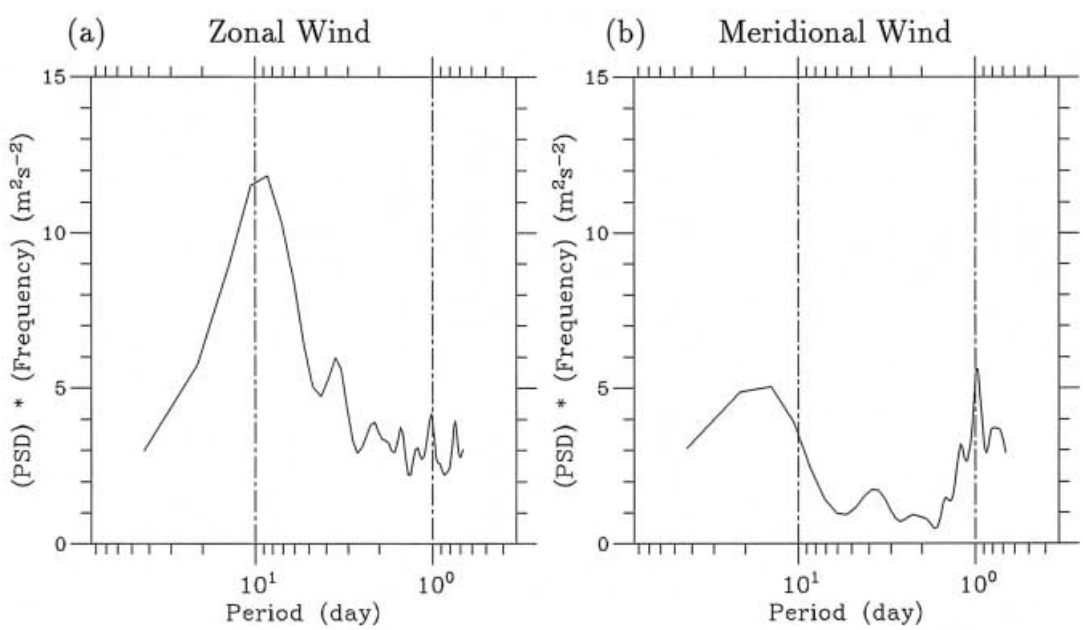

Fig. 5. Spectral analyses of: (a) BLR zonal wind; and, (b) BLR meridional wind averaged for 1–2 km height range. Vertical dashed-and-dotted lines indicate the diurnal oscillation (period of one day) and the 10-day periodicity.

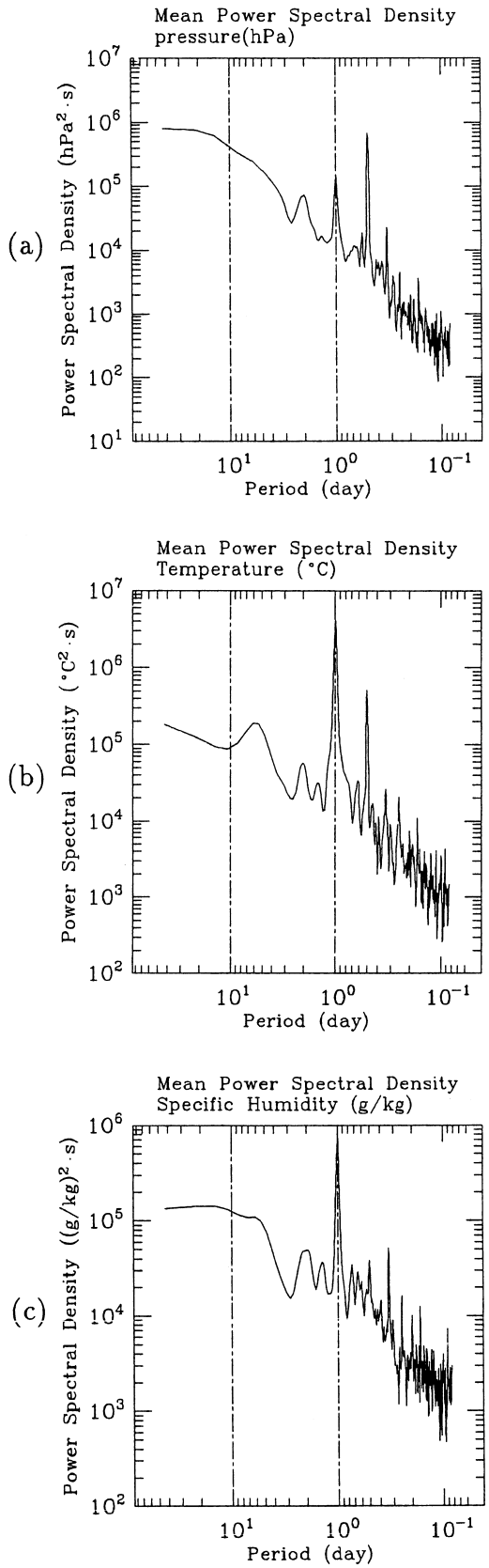

(see Section 3). The occurrence of precipitation tends to be concentrated at 12–24 LST. This result is consistent with analysis for longer periods by Hamada et al. (2002) and Renggono et al. (2001). The maximum precipitation tends to occur during 16–18 LST.

On the other hand, the quasi-10-day periodicity was weak but appeared for all the parameters. To investigate the phase relationships between these parameters, a composite analysis is made for 7–13 day filtered BLR horizontal wind (averaged for 1–2 km height range), and surface meteorological variables (pressure, temperature and specific humidity) (see Fig. 8). The reference times are taken as 6 LST on 22 September, 16 LST on 3 October and 16 LST on 11 October, corresponding to minima of zonal wind. The phase differences to the zonal wind are 1/4 cycle for the meridional wind, 5/8 cycle for the pressure, 3/8 cycle for the temperature, and 1/2 cycle for the specific humidity.

5. Comparisons with horizontal distributions of zonal wind and clouds

In order to examine the horizontal scales of the quasi-10-day components found in the preceding section, the large-scale horizontal distributions of low-level zonal wind and developed clouds are analyzed in this section.

Figure 9a compares the BLR zonal wind averaged for the height range of 0.6–1.0 km (corresponds to the altitude range of 1.5–1.9 km from MSL) with NCEP 850 hPa data at the nearest grid point (0°, 100°E) to Kototabang. Both curves are quantitatively in good agreement. The quasi-10-day periodicity can be seen also in the NCEP data as less than 2 m/s zonal winds which correspond to the weak westerly periods at Kototabang during 15 September–15 October. Thus we utilize the NCEP data to investigate the zonal structure of the quasi-10-day periodicity. Figure 9b is the time-longitude cross section of zonal wind for 40–160°E along the equator. In this figure

Fig. 6. Spectral analyses of: (a) surface pressure; (b) surface temperature; and, (c) surface specific humidity. Vertical dashed-and-dotted lines indicate the diurnal oscillation and the 10-day periodicity.

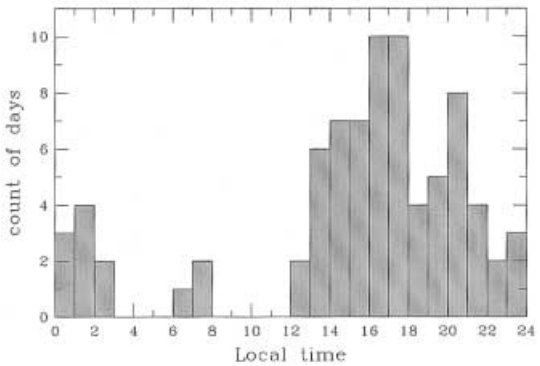

Fig. 7. A Histogram of precipitation for each hour at Kototabang during September–October 1998. The precipitations were decided by BLR.

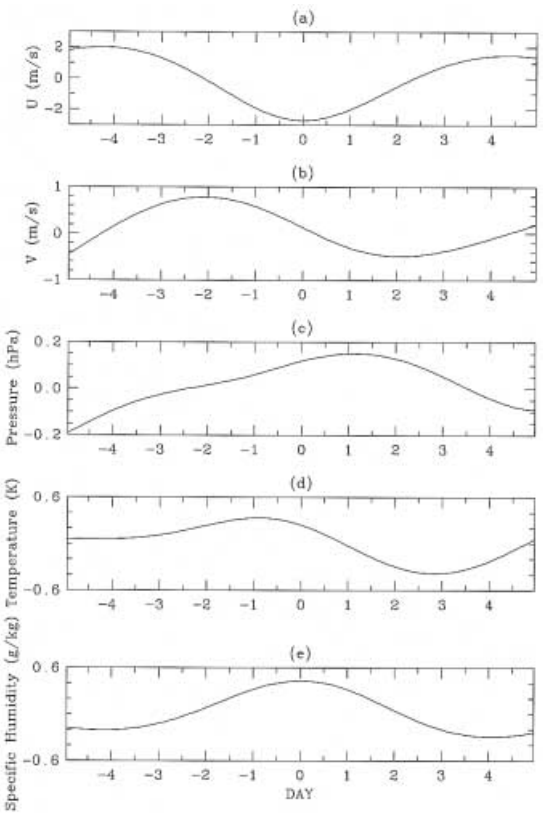

Fig. 8. Composite time series of 7–13 day filtered: (a) zonal wind by BLR averaged over 1–2 km height range; (b) meridional wind by BLR averaged over 1–2 km height range; (c) surface pressure; (d) surface temperature; and, (e) surface specific humidity. The horizontal axis represent day number from westerly wind minimum hour.

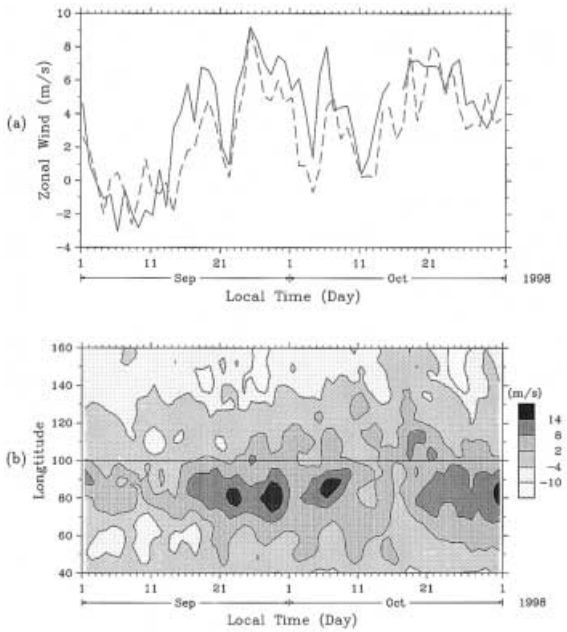

Fig. 9. (a) Time series of zonal winds. Solid curve is BLR wind averaged every 60-min, and over 0–1 km height range. Dotted curve shows NCEP 850 hPa grid point data. (b) Time-longitude cross-section of zonal wind at 850 hPa by NCEP.

strong westerly wind appears in 70–100°E during 15 September–10 October and 20–31 October. Moreover, about 10-day periodicity appears in each period. However, the correlation with the quasi-10-day periodicity at Kototabang is unclear. Another remarkable point is that these strong wind regions do not continue eastward beyond 100°E. The zonal wind field is different between the both sides of 100°E.

Next the rainfall durations at Kototabang are compared with the time-longitude cross section of the 12-hourly GMS T_{BB} data (Fig. 10). The T_{BB} data are averaged in 2.6°S–2.6°N. In this period the two large-scale disturbances appear in 80–100°E: One appears during 11 September–6 October, and the other appears during 22–31 October. However, the rainfalls at Kototabang are hardly correlated with the cloud images. This suggests a peculiarity of the precipitation at Kototabang. The T_{BB} data also show a difference between both sides of 100°E. In the western side many tall clouds are dominant. Comparing the T_{BB} data (Fig. 10b) with

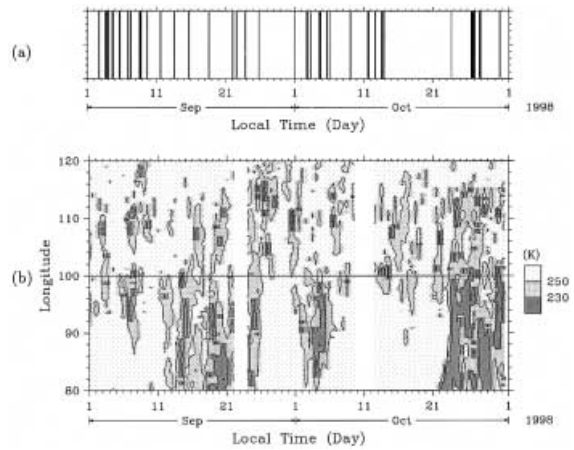

Fig. 10. (a) Rainfall durations decided by BLR, same as in Fig. 4(b). (b) Time-longitude cross-section of 12-hourly GMS IR data averaged 2.6°S–2.6°N.

the zonal wind field (Fig. 9b), the strong zonal wind fields are nearly coincident with the large-scale cloud disturbances (i.e., 11 September–10 October and 20–31 October), but the smaller scale variations have no good correlations with each other.

Figure 11 shows the composite of GMS T_{BB} data of 00 GMT and 12 GMT (corresponding to 7 LST and 19 LST, respectively) for the weak westerly periods (21–23 September, 2–4 October and 12–13 October; the data of 11 October was not used because of missing data) and the strong westerly period (16–18 September, 27–29 September and 6–8 October). There are only few clouds on Sumatera Island in the morning (see Figs. 11a and 11c), but many clouds are distributed on the mountain range which is located along the western coast in the evening (see Figs. 11b and 11d). It implies that clouds on Sumatera Island have clear diurnal variation. Figure 11 also shows that the clouds on Sumatera Island are much more active during weak westerly periods (Fig. 11d) than strong westerly periods (Fig. 11b).

6. Discussions on the precipitation-wind relationship over Sumatera mountains

At Kototabang the precipitation occurred when the low-level westerly wind became weak (Figs. 3 and 4). Both the zonal wind and the precipitation varied with quasi-10-day periodicities during 15 September–15 October (Fig. 4), and the spectral analysis showed the clear peaks around 10 days for horizontal wind of the 1–2 km height range (Fig. 5). The surface meteorological variables had weak similar features with various phase-lags (Fig. 8), although they did not have clear spectral peaks near 10 days (Fig. 6).

Over the Indian Ocean (80–100°E) the cloud activities did not have clear 10-day periodicities (Fig. 10). However, the zonal wind (70–100°E) also varied with about 10-day periodicities (Fig. 9). In general, periodicities of the tropical cloud systems have been mainly discussed in the relationship to the theoretical equatorial waves. For example, Takayabu et al. (1996) found out a quasi-2 day mode from cloud activities by GMS, rainfall data by meteorological radars, rawinsondes, a UHF wind profiler and meteorological buoy data over the equatorial Pacific, and identified it with westward propagating inertio-gravity waves. Widiyatmi et al. (1999) found out a quasi-4 day mode in the Serpong BLR data, and GMS data in rainy seasons of Java Island, and considered that it may be mixed Rossby-gravity waves propagating westward. However, these are shorter than the time scales of periodicities found in this case study.

The quasi-10-day periodicities of wind and rainfall observed at Kototabang (Fig. 4) did not well correspond to the large-scale cloud disturbances over the Indian Ocean. It seems that the longitude 100°E was a zonal boundary for the cloud systems over the tropical Indian-Pacific Ocean regions (Fig. 10). The fact implies that effects of the mountain range blocked the large-scale Indian-Ocean disturbances. Some studies have already suggested the importance of the mountain range in Sumatera Island to the large-scale cloud activity. Nitta et al. (1992) analyzed the westerly wind burst, which is considered as one of the factors that cause El Niño events, affected by Sumatera Island. It is also known that ISO is sometimes depressed near 100°E (e.g., Murakami and Matsumoto 1994).

The local-scale cloud systems along the mountain range of Sumatera in Figure 11d are considered as the cause of precipitations with the quasi-10-day periodicities at Kototabang. The cloud systems were active in the evening. The obvious diurnal variations also appear

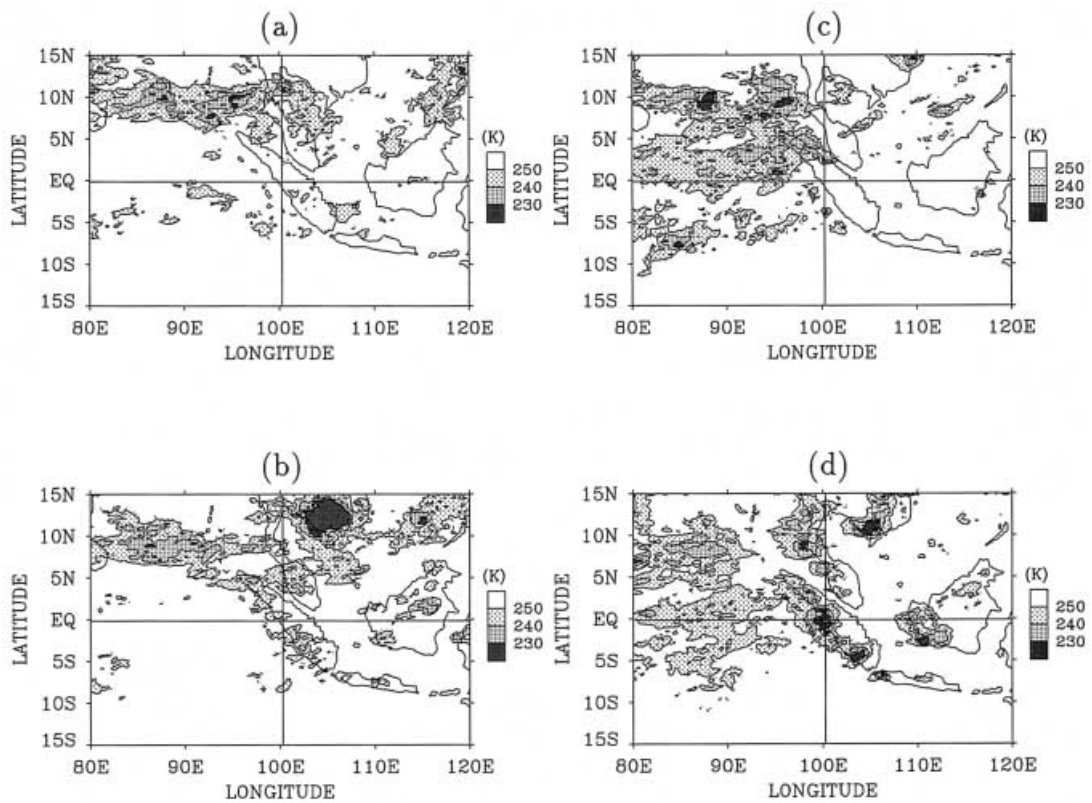

Fig. 11. Composite maps of GMS T_{BB} data for the strong westerly periods: [(a) 00 GMT and (b) 12 GMT]; and for the weak westerly periods [(c) 00 GMT and (d) 12 GMT]. 00 GMT and 12 GMT correspond to 7 LST and 19 LST, respectively.

commonly in Figs. 5b, 6 and 7. Nitta and Sekine (1994) showed from GMS IR data that diurnal variations are striking in cloud activities in/around the Indonesian maritime continent. Diurnal variations of rainfall characteristics in/around Sumatera Island have been suggested by Oki and Musiake (1994) for Malaysia, and by Hamada et al. (2002) for Indonesia. The geographical condition and the cloud distributions imply that the local-scale cloud systems had occurred by the convergence of sea breezes from the Indian Ocean and from the Strait of Malacca, or valley breezes.

Comparison between Figure 11b and 11d represent that the local-scale cloud systems had suppressed during the strong westerly periods. It is generally thought that local circulations are dominant under weak background winds. The development of the local-scale cloud systems themselves may have been controlled by the strength of the background wind.

7. Conclusions

In this paper, the observational results at Kototabang in Sumatera mountain range during September and October 1998 (rainy season) concerning the relationship between precipitation and other meteorological variables, mainly zonal wind, have been described. Estimation of rainfall durations based on BLR echoes has been successfully applied, by which we described rainfalls continuously throughout the two months with high temporal resolution. The observation showed that the precipitation at Kototabang tended to occur when the low-level westerly wind became weak, and that the westerly wind varied with a quasi-10-day periodicity during 15 September and 15 October.

The precipitation at Kototabang was not correlated with the large-scale cloud disturbances which were active only over the Indian Ocean, located in the western side of longitude 100°E. It implies that effects of the mountain range of Sumatera blocked the large-scale cloud disturbances on the Indian Ocean. The precipitation at Kototabang was caused mainly by the diurnally oscillating, local-scale cloud systems along the mountain range. It is considered that the cloud systems developed from the convergences of local circulations, and were possibly suppressed by the strong background westerly wind.

In conclusion, this study has described the observational results during September–October 1998, and discussed possible mechanisms of cloud activities on Sumatera from generalized information. The focus of this study was the cloud activities over the tropical mountainous region where clouds are in general considered to be easily generated by local circulations under usual conditions. This point is somewhat different from almost all the foregoing tropical cloud studies, which mainly considered mechanisms to enhance cloud activities over the ocean mainly by equatorial waves.

Acknowledgements

The authors express their hearty thanks to Mr. Sri Diharto, Director General of BMG for his kind permission to use the GAW Observatory for our collaborative observations. The authors are grateful to Ms. Noriko Okamoto, Mr. Findy Renggono and other colleagues of BPPT, BMG, University of Tokyo, Kyoto University and Kobe University for their cooperation for the intensive observation. The authors thank Mr. Nasrullah and the other staff members at Kototabang GAW Station for providing the surface measurement data. Thanks are due to Dr. Teruo Ohsawa and Mr. Noriyuki Nishi for providing the GMS T_{BB} data and for helpful comments. The authors are grateful to Mr. Jun-Ichi Hamada, Mr. Yoshihiro Tomikawa, Dr. Tomoe Nasuno and Dr. Yukari N. Takayabu for their helpful discussions and to Dr. Yoshiaki Shibagaki and Dr. Jun Matsumoto for reading the manuscript carefully. Positive comments offered by the Editor (Prof. H. Uyeda) and two anonymous reviewers are also greatly acknowledged.

References

Gage, K.S., 1990: Radar observations of the free atmosphere: Structure and dynamics, *in Radar in Meteorology: Battan Memorial and 40th Anniversary Radar Meteorology Conference*, edited by D. Atlas, American Meteorological Society, pp. 534–565.

Hamada, J.-I., M.D. Yamanaka, J. Matsumoto, S. Fukao, P.A. Winarso and T. Sribimawati, 2002: Spatial and temporal variations of the rainy season over Indonesia and their link to ENSO. *J. Meteor. Soc. Japan*, **80**, (in press).

Hashiguchi, H., S. Fukao, T. Tsuda, M.D. Yamanaka, D.L. Tobing, T. Sribimawati, S.W.B. Harijono and H. Wiryosumarto, 1995: Observations of the planetary bounbary layer over equatorial Indonesia with an *L*-band clear-air Doppler radar: initial results. *Radio Sci.*, **30**, 1043–1054.

———, S. Fukao, M.D. Yamanaka, S.W.B. Harijono and H. Wiryosumarto, 1996: An overview of the planetary boundary layer observations over equatorial Indonesia with an *L*-band clear-air doppler radar. *Beitr. Phys. Atomosph.*, **69**, 13–25.

Holton, J.R., 1992: An introduction to dynamic meteorology. 3rd ed. Academic Press, 511pp.

Lau, K.M., L. Peng, C.H. Sui and T. Nakazawa, 1989: Dynamics of super cloud clusters, westerly wind bursts, 30–60 day oscillations and ENSO: an unified view. *J. Meteor. Soc. Japan*, **67**, 205–219.

Madden, R.A. and P.R. Julian, 1971: Detection of a 40–50 day oscillation in the zonal wind in the tropical pacific. *J. Atmos. Sci.*, **28**, 702–708.

Murakami, T. and J. Matsumoto, 1994: Summer monsoon over the Asian continent and western north pacific. *J. Meteor. Soc. Japan*, **72**, 719–745.

Nakazawa, T., 1988: Tropical super cloud clusters within intraseasonal variations over the western pacific. *J. Meteor. Soc. Japan*, **66**, 823–839.

Nitta, Ts. and S. Sekine, 1994: Diurnal variation of convective activity over the tropical western pacific. *J. Meteor. Soc. Japan*, **72**, 627–641.

———, T. Mizuno and K. Takahashi, 1992: Multiscale convective systems during the initial phase of the 1986/87 El Niño. *J. Meteor. Soc. Japan*, **70**, 448–466.

Oki, T. and K. Musiake, 1994: Seasonal change of the diurnal cycle of precipitation over Japan and Malaysia. *J. Appl. Meteor.*, **33**, 1445–1463.

Renggono, F., H. Hashiguchi, S. Fukao, M.D. Yamanaka, S. Ogino, N. Okamoto, F. Murata, B.P. Sitorus, M. Kudsy, M. Kartasasmita and G. Ibrahim, 2001: Precipitating clouds observed

by *L*-band boundary layer radars in equatorial Indonesia. *Annales Geophysicae*, **19**, 889–897.

Takayabu, Y.N., K.M. Lau and C.H. Sui, 1996: Observation of a quasi-2-day wave during TOGA COARE. *Mon. Wea. Rev.*, **124**, 1892–1913.

———, 1994: Large-scale cloud disturbances associated with equatorial waves. part 1: spectral features of the cloud disturbances *J. Meteor. Soc. Japan*, **72**, 433–449.

Widiyatmi, I., M.D. Yamanaka, H. Hashiguchi, S. Fukao, T. Tsuda, S. Ogino, S.W.B. Harijono and H. Wiryosumarto, 1999: Quasi 4 day mode observed by a boundary layer radar at Serpong (6°S, 107°E), Indonesia. *J. Meteor. Soc. Japan*, **77**, 1177–1184.